Dendritic and Fractal Patterns in Electrolytic Metal Deposits

Yasuji Sawada,[a] A. Dougherty, and J. P. Gollub

Physics Department, Haverford College, Haverford, Pennsylvania 19041, and Physics Department,
University of Pennsylvania, Philadelphia, Pennsylvania 19104

Pattern formation in the electrodeposition of Zn from a thin layer of $ZnSO_4$ solution was studied as a function of electrolyte concentration and applied voltage. We found several qualitatively different growth forms in this system. Most strikingly, a transition from dendritic crystals (where crystalline anisotropy dominates) to disordered ramified patterns is found when the electrolyte concentration is reduced. The disordered patterns may be described as fractal below a concentration-dependent cutoff length.

The growth of dendritic crystals has attracted scientific interest for nearly half a century because the resulting symmetrical but complex forms are not well understood.[1] The complexity of dendritic growth has been identified as being due to the Mullins-Sekerka morphological instability,[2] which renders a growing interface unstable with respect to spatially periodic undulations. Since the full nonlinear problem is difficult to solve (even numerically), interest has centered on certain simplified models and limiting cases.[3-5] One fascinating discovery is that transitions from ordered dendritic patterns to more disordered ("tip-splitting") patterns may occur as the parameters representing crystalline anisotropy and supersaturation are varied.

On the other hand, deposition by diffusion to interfaces can lead to fractal patterns or aggregates, such as those produced by diffusion-limited–aggregation models.[6] These are quite different from dendrites, in that there is often no evidence of preferred axes, and the surface is rough on a wide range of scales. The possible connections between ordered interfacial patterns and fractals have been explored to a limited extent both theoretically[7-9] and experimentally through a hydrodynamic analog.[10] In this paper, we present an experimental study of the electrodeposition of zinc metal in a thin layer. We show that dendrites and several distinct disordered patterns can be realized simply by change of parameters.

The experimental configuration is a thin layer of $ZnSO_4$ solution confined between Plexiglas disks of diameter 15 cm. The gap is 0.25 mm and is uniform to within about 5%. A circular Zn electrode of diameter 10 cm surrounds the fluid, and a small carbon electrode of diameter 0.5 mm protrudes vertically into the fluid through a small hole at the center of the upper disk. This configuration differs substantially from an earlier experiment on Zn electrodeposition[11] in which the growth occurred at the interface between two immiscible fluids in a deep cell. We chose the present configuration in order to achieve a well-defined two-dimensional growth process.

The electrolyte concentration C was varied from

$0.0025M$ to $1M$ and the applied potential difference ΔV across the cell was varied from 2 to 12 V. We found that the current through the cell was linear in ΔV to within about 10% in all cases, so that the transport is essentially Ohmic. Deposits that formed on the carbon electrode over times ranging from minutes to hours were recorded on videotape and analyzed subsequently. (The competing process of electrolysis did not appear to be significant except at very low C.) We found four qualitatively distinct growth regimes as C and ΔV were varied. These regimes are summarized in the phase diagram of Fig. 1, which is based on the growth of approximately sixty patterns with parameters located at most combinations of the labeled values of C and ΔV.

(a) At the lowest C (below about $0.01M$) and low ΔV, the deposits are ramified structures with an outer boundary that remained circularly symmetric (especially at low ΔV) during the entire growth period. We call these homogeneous patterns and describe them quantitatively later. An example is shown in Fig. 2. As the concentration is further reduced, these structures begin to resemble those of DLA.

(b) At high C (roughly $0.1M-1M$) and low ΔV, the patterns grow slowly, and open ramified deposits are
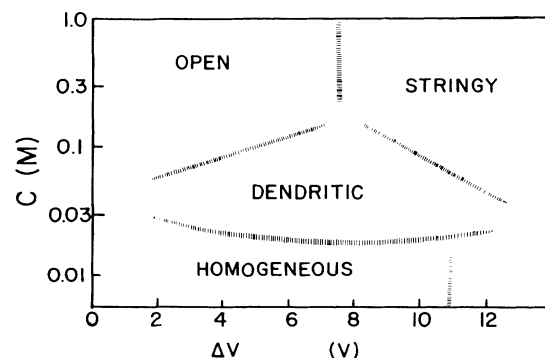

FIG. 1. Phase diagram showing the various types of patterns observed as a function of electrolyte concentration C and applied voltage ΔV.
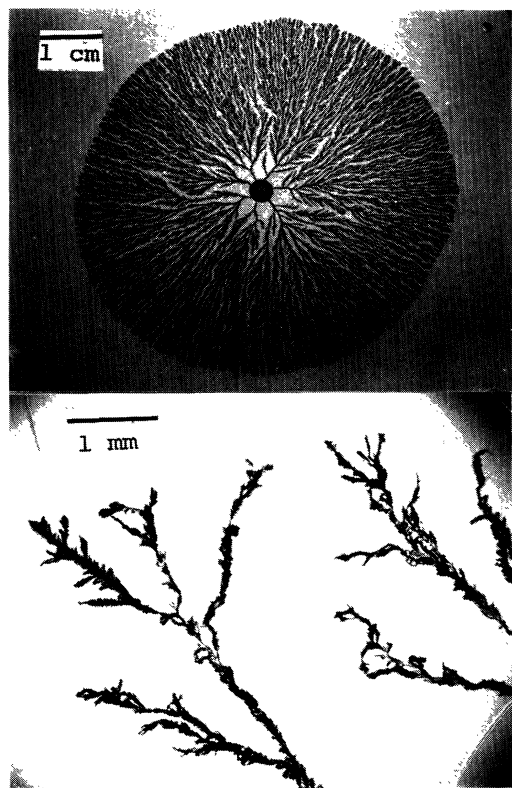
FIG. 2. Homogeneous pattern produced by the tip-splitting instability, at two different magnifications $(C = 0.01M, \Delta V = 6 \text{ V})$.

FIG. 3. (a) Open ramified deposit grown at high C and low ΔV $(C = 1M, \Delta V = 2 \text{ V})$. (b) Stringy pattern grown at higher ΔV $(C = 0.01M, \Delta V = 12 \text{ V})$.

obtained, as shown in Fig. 3(a). They appear to be roughly fractal, but are too thick to merit quantitative analysis. These patterns are similar to those studied previously.[11]

(c) At high ΔV and a wide range of C, the growth is extremely fast, and thin stringy (nonoriented) structures are obtained [Fig. 3(b)]. Here, most of the growth occurs at very few sites. The patterns resemble those produced in dielectric breakdown.

(d) Finally, there is an intermediate and rather narrow range of C that yields dendritic growth, as shown in Fig. 4(a). Here, there are well-defined "backbones" whose orientation is determined by crystalline anisotropy. In fact, these patterns are much more optically reflective than the other patterns, and each of the dendrites seems to be a single crystal. Side branches emerge from the main stems at fairly regular intervals (0.5 mm). When examined at higher magnification, we find that these dendrites have a more complex structure, as shown in Fig. 4(b). The side branches are covered with secondary side branches whose spacing is about 0.05 mm. There may also be even finer structure that is not resolved in these pictures.

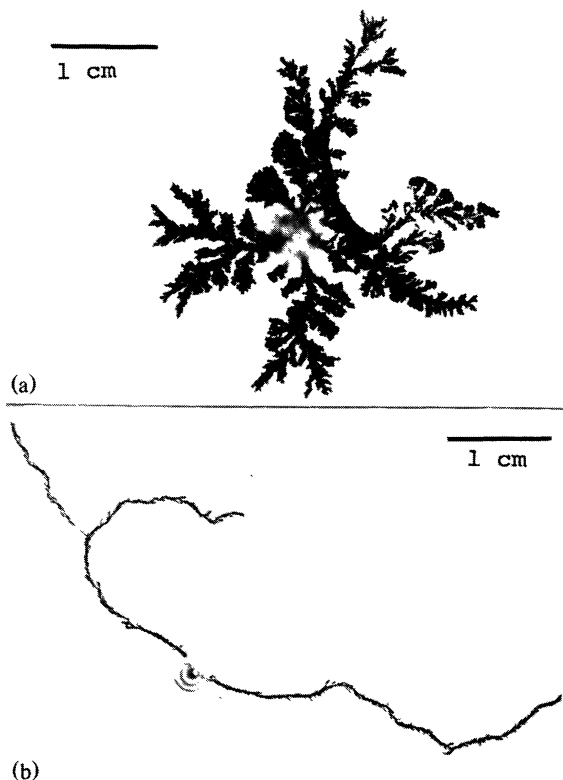The boundaries shown in the phase diagram are only

approximate. A much larger number of runs would be required to determine them accurately. This did not seem worthwhile for two reasons. First, the diagram depends to some extent on the layer thickness and on the ambient temperature (23–25 °C in our experiments). Second, the locations of the boundaries are not sharply defined, since the patterns can be inhomogeneous. For example, stringy regions are found close to the center of the homogeneous patterns [see Fig. 2(a)], presumably because the local field gradients are high there. To avoid ambiguity, our classification is based on the nature of the pattern 1.5 cm from the center.

Examination by electron microscopy showed the deposits to be thinner than 0.2 μm in cases (a) and (d). Thus, the homogeneous and dendritic patterns may be reasonably regarded as two dimensional. On the other hand, the deposits of cases (b) and (c) are much thicker (about 0.1 mm). [The open deposits (b) are composed of randomly oriented hexagonal platelets a few microns in diameter.]

Some insight into these qualitatively distinct regimes can be obtained by comparison of the linear growth speeds (Fig. 5) for various patterns, measured at the outermost part when it is about 1.5 cm from the
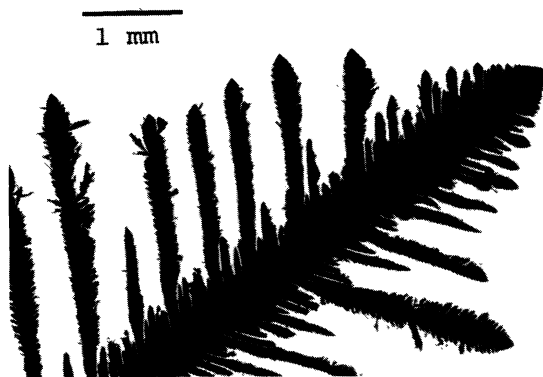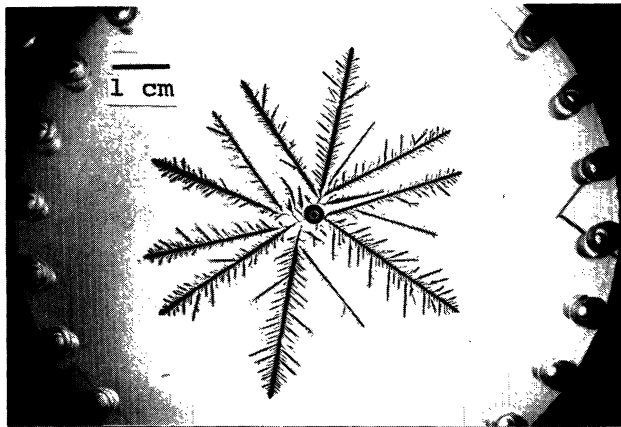
1 cm

1 mm

FIG. 4. Dendritic pattern found at intermediate concentrations ($C = 0.03M$, $\Delta V = 6$ V).
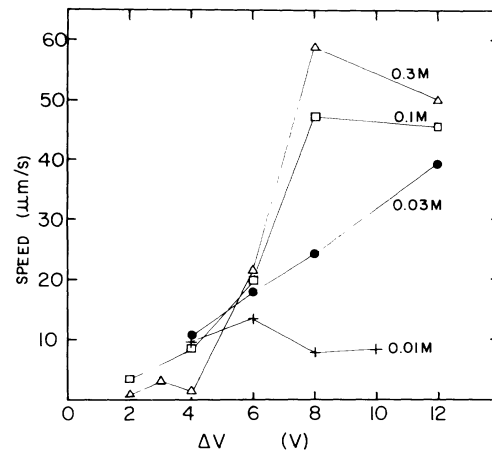

FIG. 5. Linear growth speeds for all the patterns, measured when the outermost portion of each one is 1.5 cm from the center, as a function of C and ΔV.

center. At low C (homogeneous patterns), the velocity is approximately independent of ΔV. This contrasts sharply with the behavior at high C, where the growth speed is strongly nonlinear in ΔV. In that case, the growth is extremely slow and roughly fractal deposits are formed if ΔV is low, while fast-growing stringy patterns occur if ΔV is high. Finally, we note that the growth speed is quite linear in the voltage for the dendritic case ($0.03M$).

We analyzed the homogeneous patterns quantitatively by digitization with a resolution of 512×480 pixels. The growth zone was found to be confined to the outer 10% (approximately) of the pattern. We measured the fractal dimension by dividing the pattern into boxes of size ϵ, and then counting the number of boxes containing occupied pixels as a function of ϵ, in the usual way. This number scales as ϵ^{-D}, where D is the fractal dimension. A well-defined scaling range was not found. Instead, there appears to be a crossover from a large value $D = 1.8 \pm 0.2$ at scales larger than a concentration-dependent length δ to a much smaller value of roughly 1.4 ± 0.2 at smaller scales. The patterns may be regarded as fractal on scales below δ (but above some microscopic lower cutoff),

and as approximately homogeneous on larger scales (hence the name). The length scale δ is only about 1 mm in Fig. 2, but increases strongly as the concentration is reduced. At a concentration of $0.005M$, δ is sufficiently large (about 1 cm) that the patterns resemble typical DLA patterns (they show larger gaps of variable size between growing branches than those seen in Fig. 2).

What theoretical framework is appropriate for efforts to explain these phenomena? It is well established that electric charge neutrality can be assumed, except within a thin boundary layer at the surface of the metal deposit.[12] The thickness of this boundary layer is of the order of 10 Å for a static system, but here it might be thicker, possibly of the order of the diffusion length given by the ratio of the diffusion constant to the interfacial velocity. This length would typically be tens of microns. Outside the boundary layer, the electric potential is determined by Laplace's equation. (Certain DLA models can also be regarded as generators of solutions to Laplace's equation.) The rate of mass transport outside the boundary layer is simply proportional to the gradient of the potential and to the concentration of the transported species (Zn). We believe that transport by diffusion can be neglected outside the boundary layer, because the cell is Ohmic, as explained earlier. We have also checked for macroscopic fluid motion in the cell by searching for enhanced transport of a neutral soluble dye. Motion on scales larger than the layer depth was not detected at moderate C and ΔV. However, motion on the scale of the layer depth near the interface may possibly be present. The release of latent heat is one mechanism that could induce such motion, and electric-field–induced bulk motion is also known. Therefore, the ionic transport near the surface could involve a mixture of diffusion, bulk convective motion, and

field-driven motion. This complexity may make it unrealistic to seek a quantitative model for all of the growth forms of Figs. 2–4. However, we believe that the transition from homogeneous to dendritic patterns as the concentration is varied should be amenable to theoretical treatment.

We wish to emphasize the essential observation that the transition from disordered to dendritic forms generally involves an increase in growth speed. For example, one can go from homogeneous (tip-splitting) patterns to dendrites by increasing C (and indirectly, the growth speed) at a fixed $\Delta V = 8$ V. This behavior is consistent with theoretical expectations and the behavior of simple model systems, for example, the "geometrical model" of crystal growth,[3] in which the local growth speed is taken to be a function of the local curvature. Numerical and analytical studies of this model reveal a transition to dendritic behavior as the supersaturation S (or growth speed) is increased. If S is lower than a critical value, a tip-splitting instability prevents the formation of regular dendritic patterns. Similar transitions have been observed in other simulations.[9,13] Tip splitting has been observed in ordinary crystal growth, but dendrites seem to be much more robust in that case.

During the preparation of this manuscript, we became aware of related experiments by Grier *et al.*[14] They also observe the dendritic to fractal transition as C is reduced, but classify the various patterns somewhat differently.

These observations support the existence of a close relationship between dendritic patterns that are dominated by crystalline anisotropy, and disordered patterns that may in some cases be considered to be fractal, as suggested by several theoretical models. This work leaves several important questions unanswered. What is the origin of the concentration-dependent crossover length scale δ? Why is crystalline anisotropy manifested macroscopically only in a relatively narrow part of the parameter space?

(a)Permanent address: Research Institute of Electrical Communication, Tohoku University, Sendai 980, Japan.

[1]J. S. Langer, Rev. Mod. Phys. **52**, 1 (1980), and references therein.

[2]W. W. Mullins and R. F. Sekerka, J. Appl. Phys. **34**, 323 (1963), and **35**, 444 (1964).

[3]R. C. Brower, D. A. Kessler, J. Koplik, and H. Levine, Phys. Rev. A **29**, 1335 (1984); D. A. Kessler, J. Koplik, and H. Levine, Phys. Rev. A **30**, 3161 (1984), and **31**, 1712 (1985).

[4]E. Ben-Jacob, N. Goldenfeld, J. S. Langer, and G. Schoen, Phys. Rev. A **29**, 330 (1984); E. Ben-Jacob, N. Goldenfeld, B. G. Kotliar, and J. S. Langer, Phys. Rev. Lett. **53**, 2110 (1984).

[5]W. van Saarloos and J. D. Weeks, Phys. Rev. Lett. **55**, 1685 (1985).

[6]T. A. Witten and L. M. Sander, Phys. Rev. Lett. **47**, 1400 (1981), and Phys. Rev. B **27**, 5686 (1983).

[7]T. Vicsek, Phys. Rev. Lett. **53**, 2281 (1984).

[8]L. P. Kadanoff, J. Stat. Phys. **39**, 267 (1985).

[9]L. M. Sander, P. Ramanlal, and E. Ben-Jacob, to be published.

[10]E. Ben-Jacob, R. Godbey, N. Goldenfeld, J. Koplik, H. Levine, T. Mueller, and L. M. Sander, Phys. Rev. Lett. **55**, 1315 (1985).

[11]M. Matsushita, M. Sano, Y. Hayakawa, H. Honjo, and Y. Sawada, Phys. Rev. Lett. **53**, 286 (1984).

[12]J. O'M. Bockris and A. K. N. Reddy, *Modern Electrochemistry, Vol. 2* (Plenum, New York, 1970), p. 623ff.

[13]N. Goldenfeld, private communication.

[14]D. Grier, E. Ben-Jacob, R. Clarke, and L. M. Sander, following Letter [Phys. Rev. Lett. **56**, 1264 (1986)].
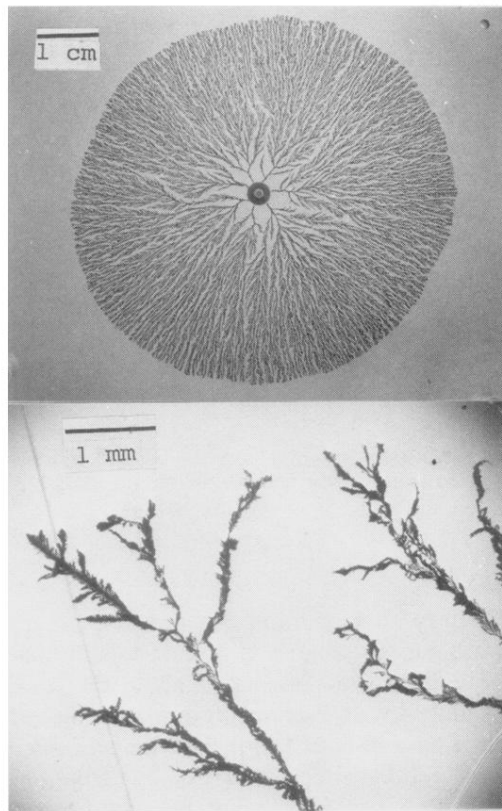
FIG. 2. Homogeneous pattern produced by the tip-splitting instability, at two different magnifications ($C = 0.01M$, $\Delta V = 6$ V).
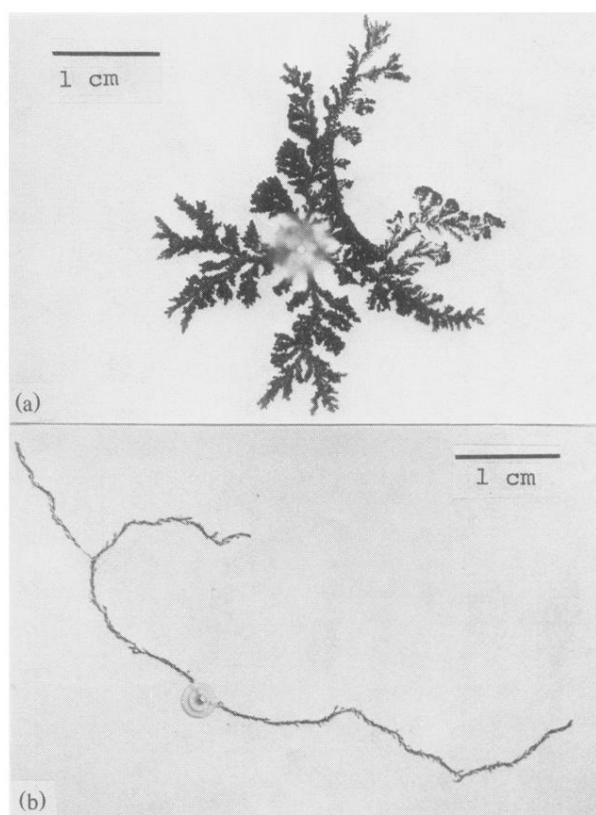
FIG. 3. (a) Open ramified deposit grown at high C and low ΔV ($C = 1M$, $\Delta V = 2$ V). (b) Stringy pattern grown at higher ΔV ($C = 0.01M$, $\Delta V = 12$ V).
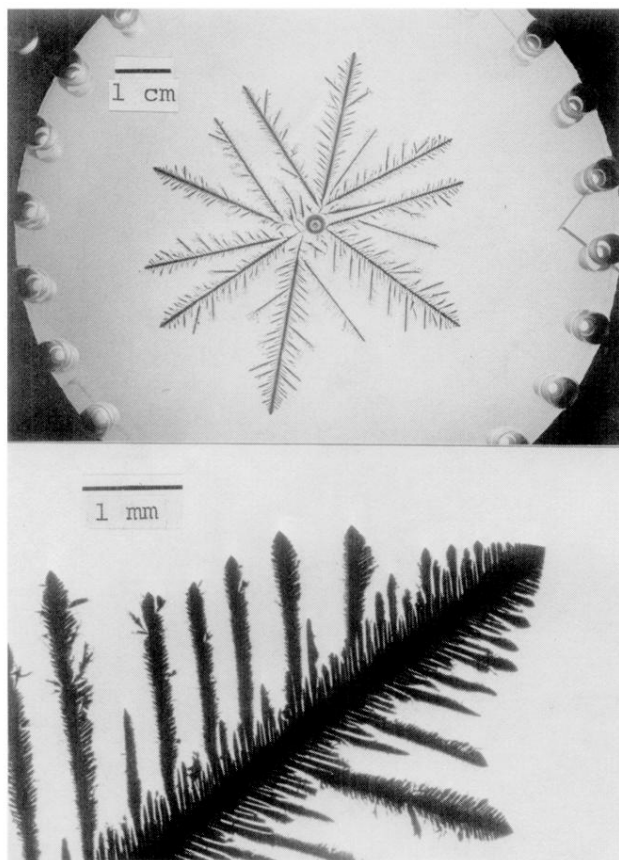
FIG. 4. Dendritic pattern found at intermediate concentrations ($C = 0.03M$, $\Delta V = 6$ V).